# Skipper - An Innovative U.S. And Russian University Space Science Mission

Deborah A. Levin
Institute for Defense Analyses
Alexandria, VA 22311

Leonard H. Caveny
Innovative Science and Technology
Ballistic Missile Defense Organization
Washington, DC 20301-7100

David M. Mann
Army Research Office
Research Triangle Park, NC 27709-2211

David A. Burt
Space Dynamics Laboratory
Utah State University
Logan, UT 84322-4140

## ABSTRACT

Skipper is the third space experiment in the Bow Shock series to obtain aerothermochemistry and emission data from shock-heated layers. Onboard instrumentation will include two scanning spectrometers and 20 photometers. The spectrometers will scan over the range of 0.2 to 0.4 μm. The photometers will be designed to view the VUV and UV wavelengths with emphasis on atomic oxygen, Lyman-alpha, NO, OH, and $N_2^+$ wavelengths. The mission starts with launch into a 822 km circular orbit at 97° inclination. Utah State University designed Skipper with their instrumentation module integrated on top of the Russian spacecraft bus. After spacecraft checkout in the 822 km orbit, the satellite uses hydrazine engines to change to an elliptical orbit with a perigee of about 180 km and begins the scientific measurements. The experimenters will then lower the perigee farther (in approximately 10 km steps) to increase the signal to noise ratios, as drag and thermal limits permit. These experiments will be completed in a two week period, followed by positioning the satellite for reentry over a Pacific test range. Additional data will be collected during the reentry (until the satellite burns up) using both onboard instrumentation and ground observation systems. Thermal modeling predicts that data can be collected down to about 80 km (at a speed of 7 km/sec).

## 1. INTRODUCTION

Skipper is a 250 kg instrument satellite designed to obtain aerothermochemistry and spectral emissions data. It is scheduled for launch during the summer of 1995 from Baikonur as a secondary payload on a Molniya launch system. Skipper is the third and last of the bow shock flight series conducted by the Space dynamics Laboratories of Utah State University (SDL/USU) in Logan, Utah. The inexpensive Bow Shock 1 and 2 sounding rocket flights gathered new information on the ultraviolet (UV) emission generated by high speed vehicles at 40 to 100 km and 3.5 to 5.1 km/sec.[1] These new


0-8194-1521-9/94/$6.00

data sparked development of the Skipper mission to answer scientifically challenging questions in the 7 to 8 km/sec range. During its orbital phase, the satellite will be put into an elliptical orbit with a low perigee. In these orbits, the satellite will "skip" over the surface of the Earth's atmosphere at 150 to 130 km perigees (hence the name). This provides a significant opportunity to collect data on aerothermochemistry interactions between the satellite and the atmosphere *in an interactive process over multiple orbits.*

USU/SDL will produce the scientific instrumentation module for the mission and subcontract development of the spacecraft bus and the launch to the Moscow Aviation Institute (MAI) in Russia. The interface between USU and MAI is based on academic level scientific exchange and collaboration. MAI also brings Russian organizations such as NPO Lavochkin with significant spacecraft experience to the program. The ties to the Russian organizations are strictly commercial activities between USU/SDL and MAI, and must be approved through normal U.S. interagency channels.

Based on the data from earlier sounding rocket flights (Bow Shock Ultraviolet Flight Experiments 1 and 2) and other satellite programs the prioritization of flow regimes is transitional, continuum, and glow.[2] For speeds of 7 to 8 km/sec and a satellite nose radius of 0.5 m the transitional regime ranges from approximately 130 to 95 km. The continuum regime starts at about 95 km and extends down to vehicle destruction (~80-75 km). The high altitude glow regime is considered to start at about 140 km altitude.

The purpose of this paper is to discuss the salient aspects of the mission planning that relate to achieving the science goals associated with optical emission from the bow-shock region. The trade-offs between vehicle design, satellite communications, and science goals will be quantified.

## 2. WHY AN ORBITING PLATFORM

Sounding rocket vehicles have historically produced a wealth of data that, among other things, have assisted in the study of the earth's atmospheric properties. More recently, that experimental concept of affordable and quick fabrication time has been extended to the study of aerothermochemistry by optical emissions. Both research communities have found the sounding rocket platform sufficiently adept at carrying optical and electron microprobe instruments which can make in-situ measurements of the atmosphere or flow surrounding the vehicle. Hence local, calibrateable measurements, free of remote sensing ambiguities, have been obtained.

A major shortcoming of the sounding rocket platform is the single event and short time of the mission, which creates the inability to change instrumentation parameters in-flight. A small orbiting satellite removes this important limitation, and at the same time provides additional attractive features. A larger excited region (*i.e.*, the shocklayer) can be created because greater physical dimensions are more likely. If the orbit is adjusted, this creates an opportunity to measure radiance from three flight regimes: the free-flow ("glow"), transitional, and continuum flow regimes. The larger dimension also provides the capability to carry more instrumentation than a sounding rocket configuration.

A secondary goal of the Skipper is to learn to utilize small satellite measurement opportunities of optical emissions, yet maintain a budget appropriate to university research.

## 3. MISSION DISCUSSION AND ANALYSES

Figure 1 shows a simple schematic diagram of the planned mission for Skipper. The figure shows the satellite initially launched to a sun-synchronous orbit of about 820 km. After a few days of satellite health checkout it is put into an elliptical orbit which will make several passes to the top of the earth's sensible atmosphere. After a specified number of orbits, that are a function of the perigee heating and the acceptable risk factor, the satellite will be positioned to accommodate a controlled reentry. The perigees and the reentry occur in the dark to simplify questions of background emissions.

### 3.1 Elliptical Orbits

A number of important perigee-altitude tradeoffs have been considered. From the point of view of the science, decreasing the perigee is desirable since that corresponds to a higher glow signal. The mission complexity however grows in terms of a decreasing lifetime, increasing spacecraft heating, and a movement of the reentry path eastward. Figure 2 shows an example of a calculation of the orbital decay for an initial apogee of 820 km and a perigee of 120 km. The uncertainty and variation in model atmospheres which contributes to the calculation of spacecraft drag is mainly above 150 km.[3] Each tick mark represents an orbit. The exact coefficient of drag of the vehicle remains an uncertainty; although recent Direct Simulation Monte Carlo calculations of Moss [4] will provide an estimate. Also the use of a hydrazine propellant system should permit sufficient control and flexibility such that the drag calculational uncertainties can be corrected for in-flight to prevent premature orbital decay.

The spacecraft heating calculations of the different components is an ongoing activity. The temperature of the spacecraft dome increases as the perigee is lowered. Various thermal cooling design strategies are presently under consideration. The instrument photocathodes chosen are relatively temperature insensitive (*i.e.*, low dark count currents will be maintained) over the range of interior temperatures expected. The solar cell arrays are the most temperature sensitive component of the spacecraft; however, recent calculations and data show that the perigee heating conditions at 130 km, 8 km/sec are tolerable.

The length of the elliptical portion of the mission presently planned is about two weeks. This corresponds to two days spent at each perigee, with the perigee descending in steps of 10 km from 180 down to 130 km. The length of the orbital mission is dictated by the desire to insure flexibility, the inability to control the launch date or time (as a secondary payload), and the economics of maintaining one trained ground crew. Figure 3 shows the perigee altitude as a function of orbit number and time from the beginning of the orbital mission. Figure 4 shows the geometry and sequence of measurements and events planned. The figure shows that uplink communications with the satellite and data downlinks are planned with the worldwide Air Force Satellite Control Network as the primary option. The extensive coverage of this network provides an optional capability to the mission particularly at the lower perigee passes where it may be necessary to have real time thermocouple and optical data. Such data may be useful in making the decision whether to lower the perigee to altitudes of 130 km and below.

### 3.2 Reentry

A number of important reentry-angle trade-offs exists as well. The initial reentry angle is defined as the angle between the vehicle longitudinal axis and the horizontal at the perigee altitude for which the deorbit command is given. Our quartz window transmission calculations show that a reentry angle of about 3° provides ample UV transmission down to altitudes below 80 km.

Similar transient heating calculations were performed for the anticipated dome material of anodized aluminum dome as a function of dome thickness. The results of these calculations show that the dome thickness needs to be about 0.5 inches to survive down to 80 km altitude. This result has been confirmed with thermocouple data from the Bow Shock Flight Experiment 2. Figure 5 shows a comparison of that data and predicted dome temperatures derived from the transient heating model of Finke.[5] Hence the heating failure mode of the dome during reentry is expected to occur between 75 - 80 km altitude.

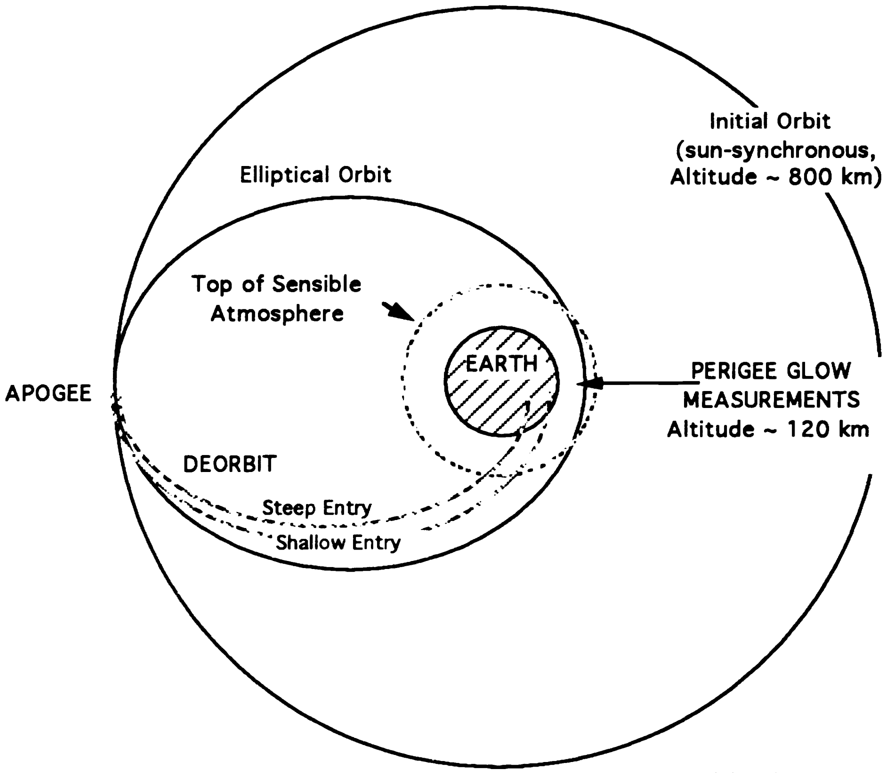


Fig. 1 Schematic diagram of orbital and reentry mission geometry (altitudes are not drawn to scale).

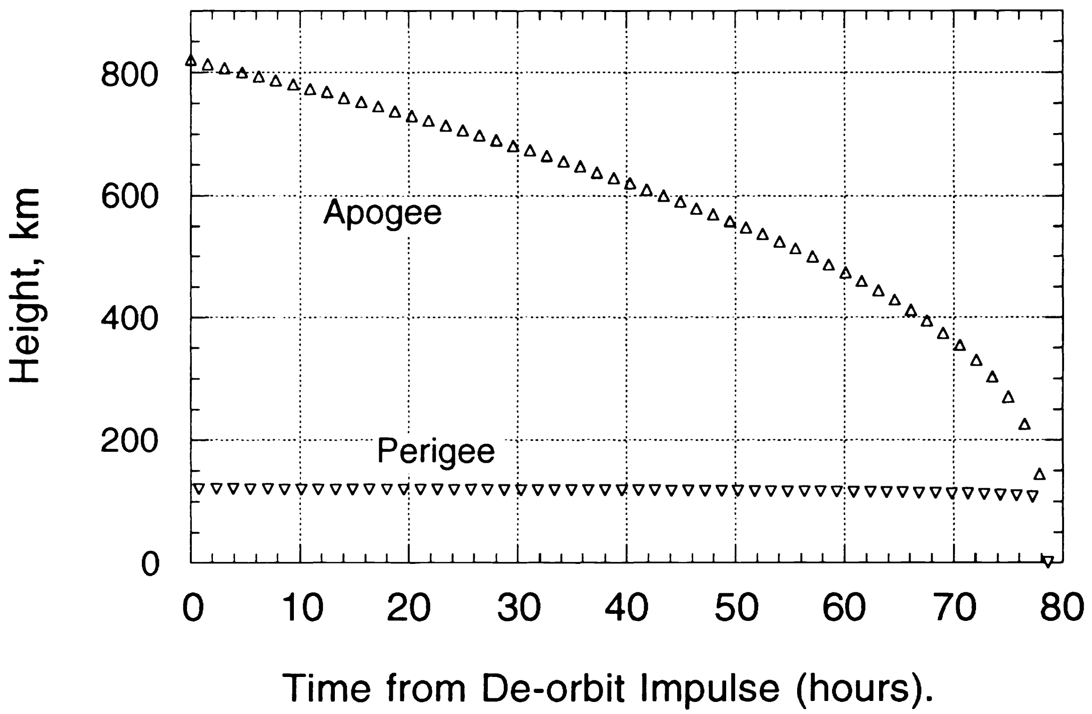


Fig. 2 Orbital decay from initial 820 x 120 - km orbit with a ballistic coefficient of 160 kg/m$^2$. Each tick mark represents a single orbit.

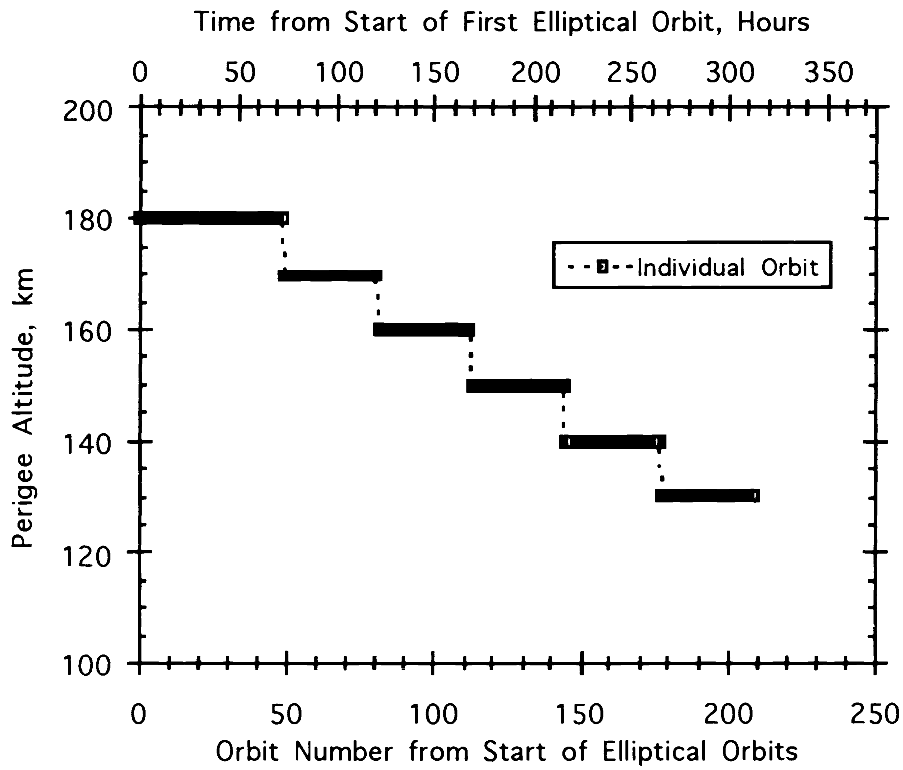


Fig. 3 Perigee altitude orbit number and time history.

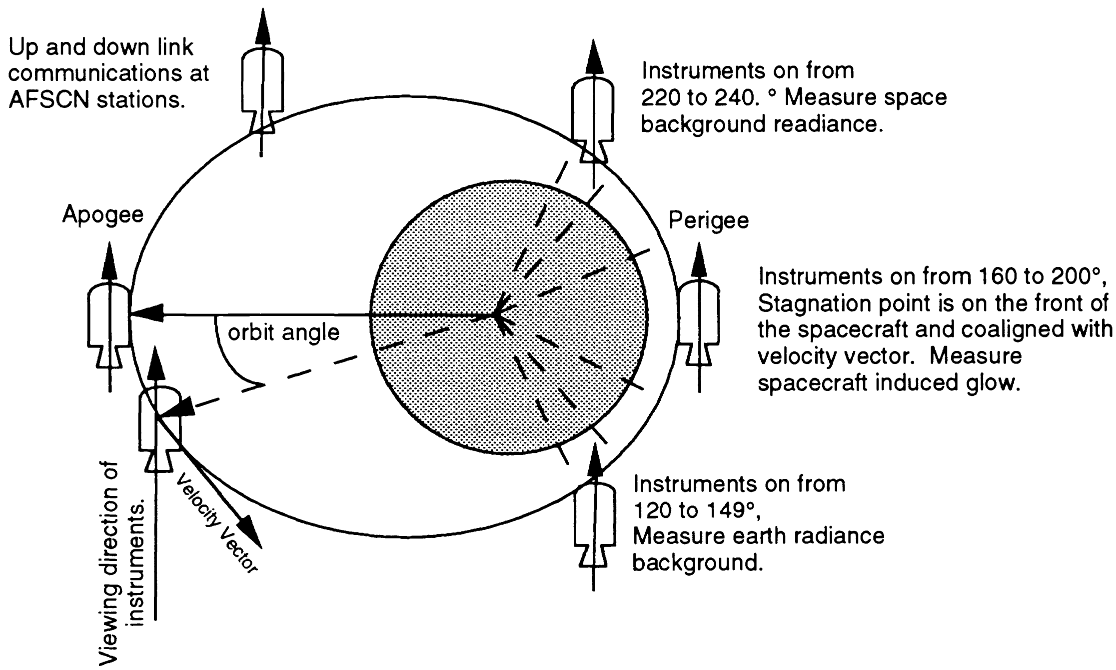


Fig. 4 Geometry and sequence of measurements and events during the elliptical orbiting portion of the mission (not drawn to scale).

The second important terminal failure mode during reentry will occur when the telemetry signal is attenuated by the surrounding bow shock plasma sheath. Hence the environment of the shocklayer in the vicinity of planned telemetry antenna for Skipper was also examined. The telemetry transponder operates at a frequency of about 2.3 GHz, which is readily available for data transmission to ground stations during the elliptical orbital phase of the mission and most reentry range facilities. A near forward antenna is located around the corner of the shocklayer - cone junction (see Fig. 6) for communication during the elliptical orbits. We also considered whether it would be possible to use that antenna-location to transmit the reentry data to a ground station during the final reentry phase of the mission.

The theory of microwave transmission[6] was been applied to a flow calculation at 80 km, 8 km/sec. Figure 7 shows the telemetry radar transmission as a function of an antenna located at different axial locations on the body for three radar frequencies. No transmission was found for a radar frequency of 2.0 GHz. There is an improvement at slightly higher frequencies and aft locations. Therefore, to extend

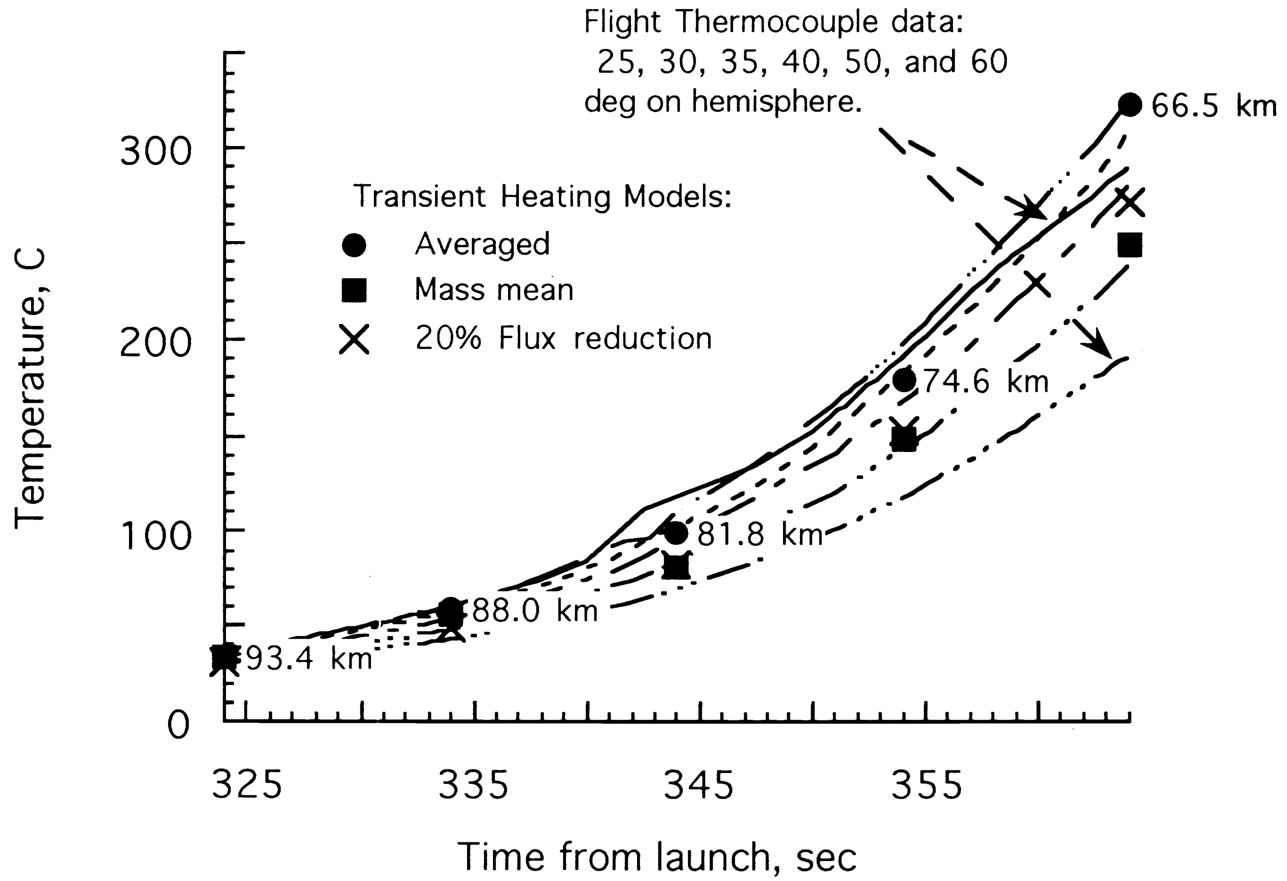


Fig. 5 Comparison of predicted and measured dome temperatures for a 10.16 cm nose radius and a speed of 5 km/sec.

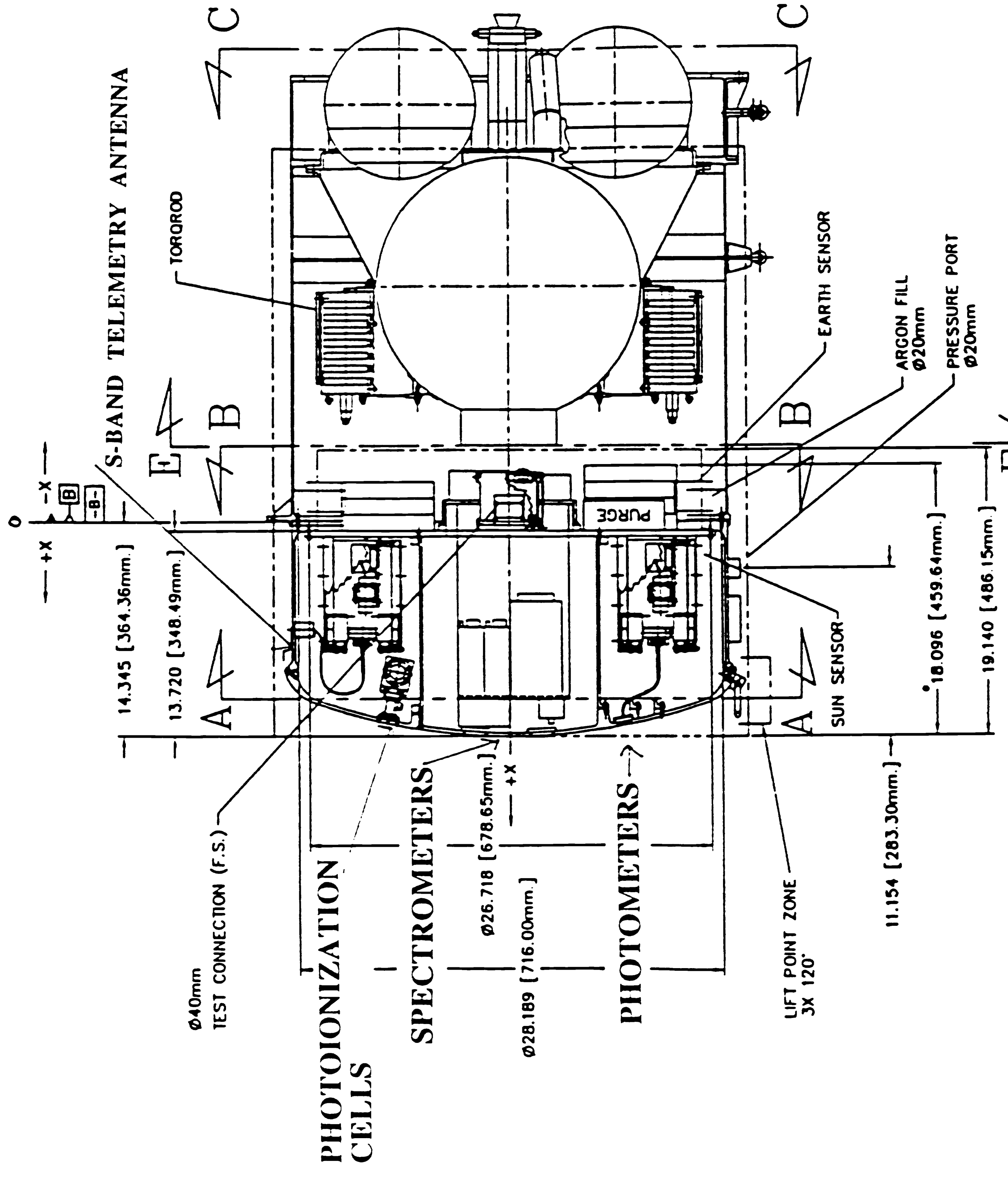


Fig. 6 General schematic diagram of Skipper payload.

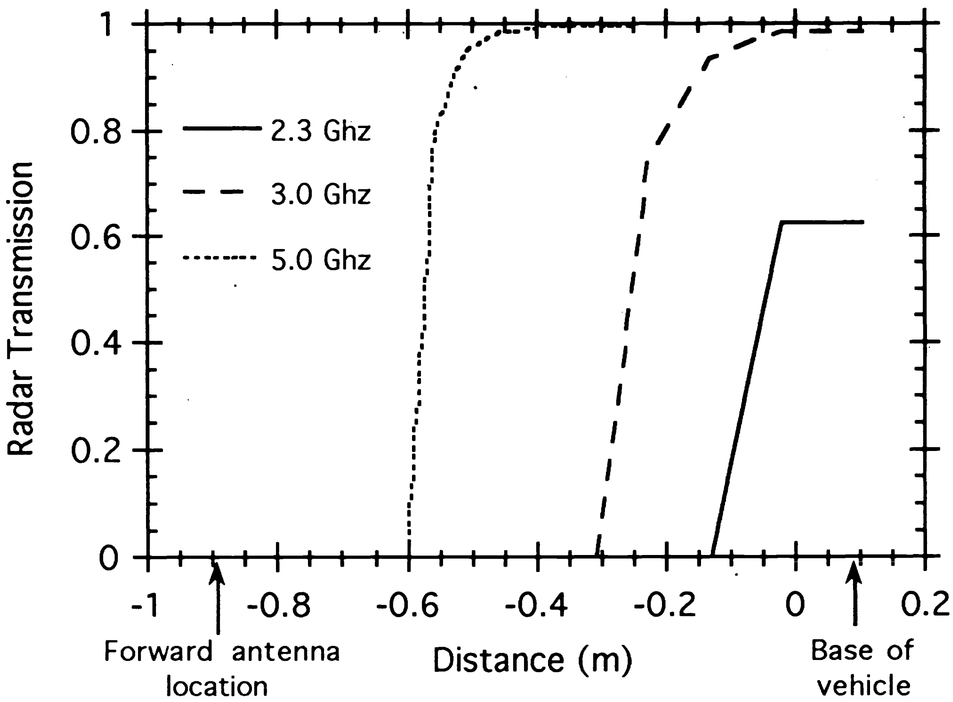


Fig. 7 Telemetry transmission as a function of antenna location along the body at 80 km

the altitude regime for which data can be collected during reentry, an additional antenna will be put at the base of the Skipper vehicle. Due to budgetary concerns the frequency will be kept at 2.3 GHz, the normal ground station operating frequency. This additional antenna also provides a more favorable line-of-sight geometry between the ground station and the satellite during reentry.

The mission is sufficiently complex that a pre-defined, quantitative decision tree is being developed. Figure 8 shows a quantitative flow-chart plan that provides a first step in obtaining that goal. In particular it provides specificity in terms of spacecraft subsystem status and decisions regarding subsequent measurements. These decision branch points need to be evaluated during the mission to incorporate the "on-orbit adaptation" philosophy of Skipper. Specific criteria for the "REASSESS" boxes are in the process of being defined with input from the Skipper Science Team.

## 4. SUMMARY OF PRE-FLIGHT RADIANCE CALCULATIONS AND PHENOMENA

### 4.1 Glow Phenomena

The phenomena will be discussed from high to low altitudes. Starting with the glow regime consider the photometric data from the Atmospheric Explorer (A. E.) Satellites.[7] The analyses of the data at altitudes above 160 km showed that the glow brightness was proportional to the free stream atomic oxygen number density; whereas, at lower altitudes (*i.e.*, 140 - 145 km) the signal levels increased

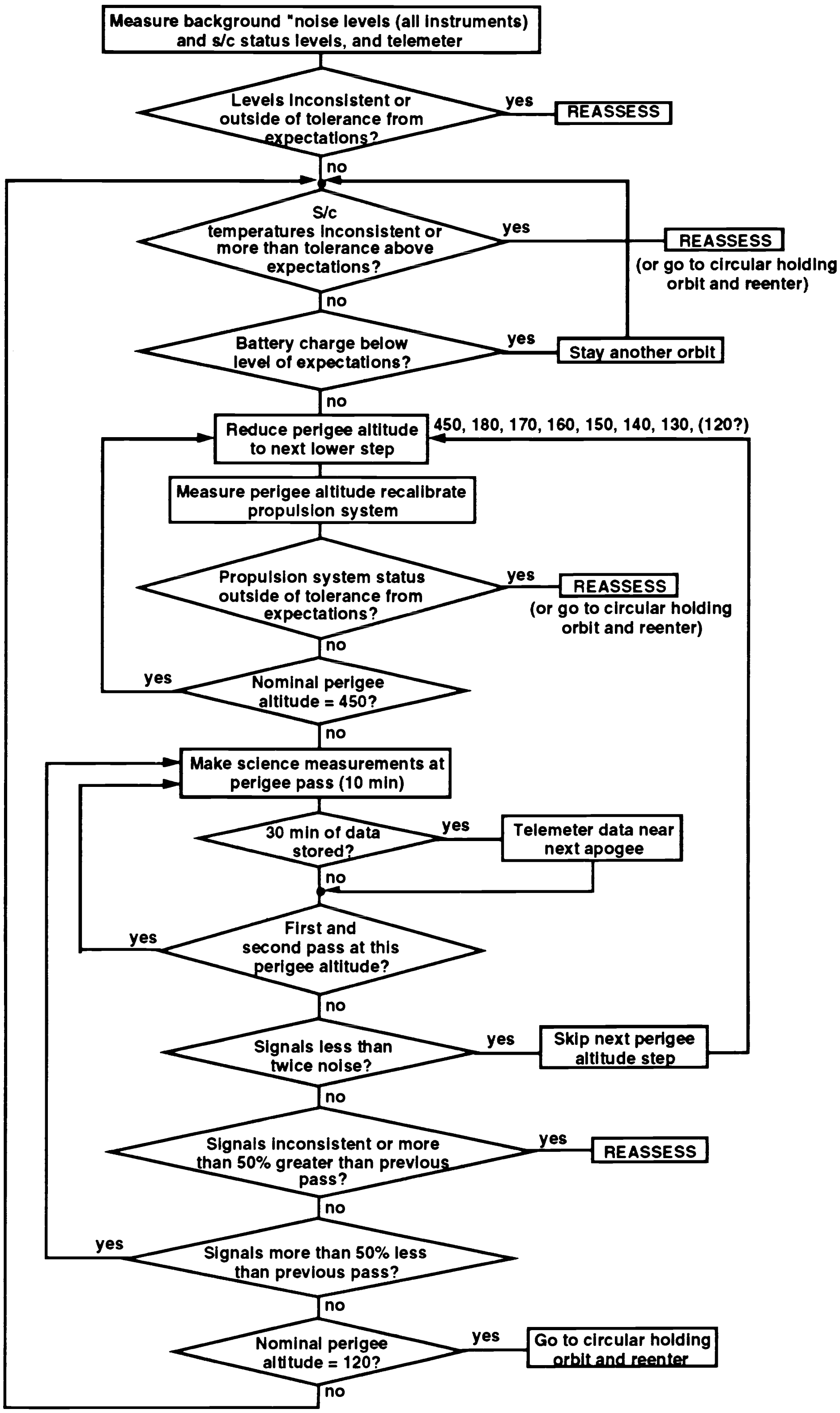


Fig. 8 Operations/ decisions flow (staring in a circular check-out orbit).

dramatically with decreasing altitude and were no longer proportional to either the free stream number density of atomic oxygen or molecular nitrogen. An understanding of the change from free-flow to the transitional regime, where a weak bow shock is formed, is required to fully interpret this data.

Whether the spectral distribution of the glow in the 140 km to 180 km altitude region observed on the A. E. Satellites was the same as that observed on the shuttle is unclear. "Shuttle glow" models[8] are based on a set of surface chemical reactions and luminescence and appear to match the observations made on the shuttle. It should be noted, however, that the measurements have been made in a "dirty environment" due to the outgassing of a large spacecraft and the contamination caused by the hydrazine rocket engines. On the simpler spacecraft, the A.E. used only five photometers and did not carry a spectrometer. The lack of spectrometers on the A.E. satellite raises the question, do the spectra from the shuttle match those inferred from the A.E. photometers? These questions influenced the selection of Skipper instrumentation.

### 4.2 Transitional and Continuum Phenomena and Pre-flight Calculations

The history and results of earlier flight programs in this speed and altitude regime have been discussed extensively in Ref. 2. The computational methods are also discussed there as well. We repeat two of the salient calculations presented there to illustrate the new phenomena that will be observed on Skipper. Additional calculations by researchers at MAI and TsIINIMash are in progress as well.[9]

Figure 9 shows the computed radiance as a function of free stream density (or altitude) for radiation in a photometer centered at 230 ± 25 nm. This photometer covers the peak spectral region of the NO molecular bands and has been used successfully on earlier flights. The different background levels are also indicated. The figure shows the overlap between the continuum[10] and transitional flow methods.[11] The continuum methods breakdown at about 100 km as the mean free path between collisions increases (with increasing altitude). The actual signal is probably a smooth line using the DSMC from 160 - 100 km and the continuum model for lower altitudes. The implied required dynamic range of the photometer can also be seen from the figure. A single photometer should be able to accommodate the required dynamic range and sensitivity; however, since this is considered a high priority measurement two photometers with overlapping sensitivities will be used.

Figure 10 shows a computed spectra at 80 km for resonance and non-resonance VUV transitions.[12,13] The total spectra as well as its significant components are shown. Molecular $O_2$ radiation was found not to contribute. The calculation of the VUV radiation is computationally intensive. Hence the absolute magnitude of the peak heights shown in the calculated spectra (Fig. 10) may be too low by a factor of two. The spectra is characterized by the presence of atomic O and N atomic lines superimposed on a molecular continuum of $N_2$ and NO. It is also interesting to note the importance of the NO ε band system, *i.e.*, NO (D → X).from about 170 - 200 nm.

## 5. INSTRUMENTATION

Table 1 shows a summary of the characteristics of the twenty photometers that will be carried on Skipper. When more than one photometer is indicated, each one will have a different sensitivity level so that the anticipated entire dynamic range of the measurement can be accommodated. Table 1 and shows the overlap of the photometers with previous Bow Shock measurements, the Atmospheric Explorer data sets, and species of interest to interplanetary missions.

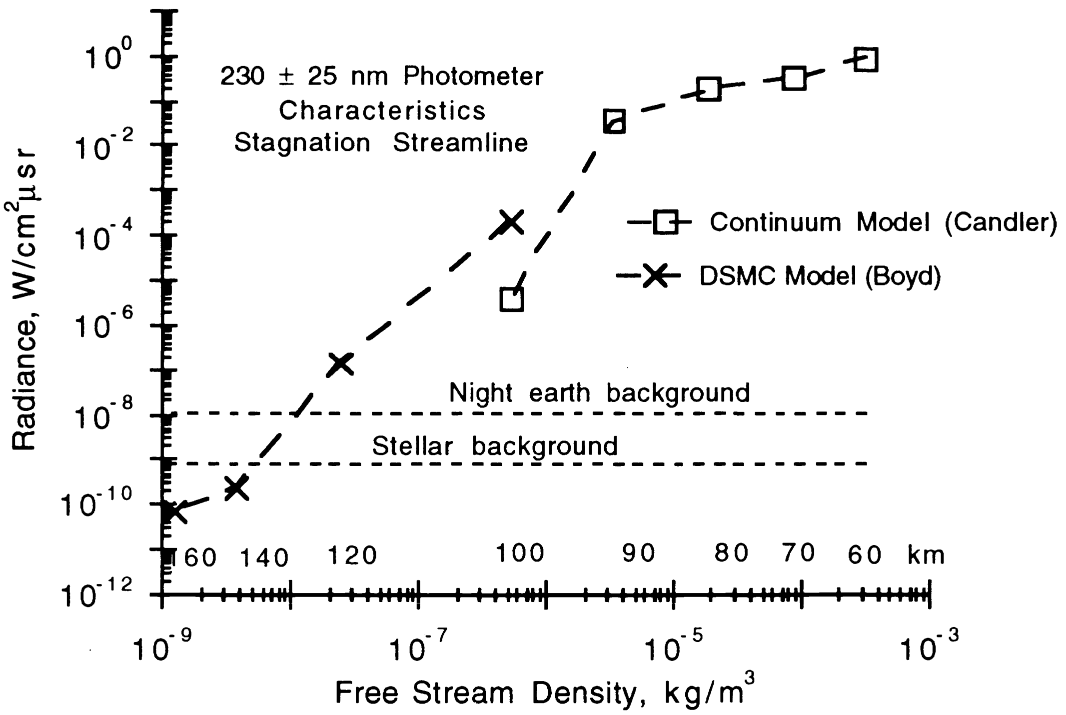


Fig. 9 Pre-flight calculations for radiance levels in the 230 ± 25 nm photometer passband.

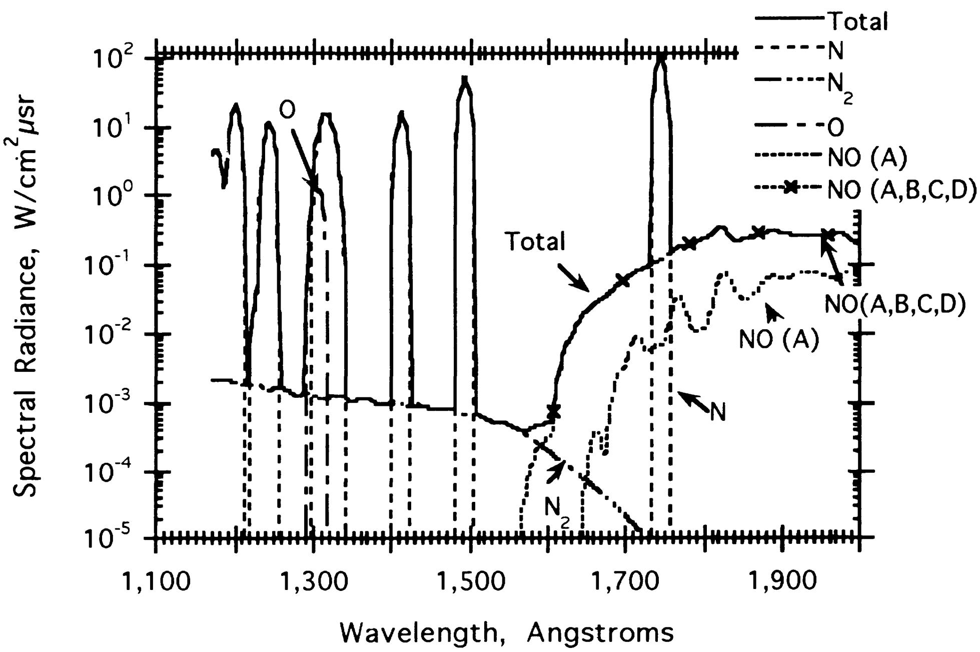


Fig. 10 Pre-flight calculations of VUV spectra at 80 km.

In addition to these photometers, four VUV photometric instruments will be flown. Two will be gas filled ionization cells similar to those flown on Bow Shock 2 with the filling gas and detector-window material chosen to be sensitive to 130 (atomic oxygen) and 121 nm (atomic nitrogen).[12] The other two cells will also be sensitive at the same wavelengths but are photon counting detectors.[14] The combined dynamic range of a ionization cell and a photon counter is about six orders of magnitude. The operating range of the 130 nm photon counter and the photoionization cell will be $10^{-8}$ to $10^{-5}$ and $10^{-5}$ to $10^{-2}$ $W/cm^2sr$, respectively. The atomic nitrogen measurements will have the same minimum sensitivity to maximum, unsaturated, range of signal levels.

The parameters of the two scanning spectrometers presently planned for the experiment are given in Table 2. A windowless VUV instrument will scan from 115.0 to 230.0 nm. A UV instrument similar to that flown on Bow Shock 2 (but about a factor of 6 more sensitive) will cover the 200.0 to 400.0 nm spectral region. The estimated sensitivity of the spectrometers is $5x10^{-10}$ $W/cm^2sr\mu m$. The inherent dynamic range of each of the spectrometers is about six orders of magnitude. To accommodate the predicted dynamic range an additional four orders of magnitude will be obtained by a combination of electronic gain changes at predetermined altitudes, and for the UV instrument the insertion of a mechanical iris.

Figure 11 shows a more detailed plan of the instrument locations, windows, and viewing geometries.

## 6. ACKNOWLEDGMENTS

The Ballistic Missile Defense Organization contracted with USU/SDL to conduct the Bow Shock 3 experiment, *i.e.,* Skipper. The design of Skipper is a collaborative university effort with USU/SDL serving as the program manager. The Moscow Aviation Institute and NPO Lavotchkin are the principal subcontractors.. USU/SDL is designing the filtered photometers and the atomic oxygen [OI λ130.4 nm] and hydrogen [HI λ121.5 nm] VUV instruments. The University of Pittsburgh is developing the rapid scanning spectrometers. TsIINIMASH will provide VUV photoionization cells. The Skipper Science Group is headed by the Army Research Office and includes U.S. and Russian participation. The Institute for Defense Analyses has a central role within the Skipper Science Group.

## 7 REFERENCES

1. D. Levin, L. Howlett, L. Caveny, and D. Mann, "High Altitude Shock-layer Ultraviolet Emissions Measured Using Highly Elliptical Orbits," *SPIE Surveillance Technologies and Imaging Components,* Vol. 1952, April 1993.
2. D. Levin, R. Finke, G. Candler, I. Boyd, C. Howlett, P. Erdman, and E. Zipf, "In-situ Measurements of Transitional and Continuum Flow UV Radiation from Small Satellite Platforms," *AIAA Paper No. 94-0248*, January, 1994.
3. A. S. Jursa, Scientific Editor, Handbook of Geophysics and the Space Environment, Air Force Geophysics Laboratory, Air Force Systems Command, United States Air Force, 1985, p. 14-27.
4. Jim Moss, NASA/ Langley Research Center, private communication.
5. Finke, R. G., "Calculation of Re-entry Vehicle Temperature History," *IDA Paper, P-2395,* September 1990.
6. J. J. Martin, Atmospheric Reentry, Prentice-Hall, Inc., N. J., 1966.

Table 1. Photometer Assignments

| Feature/ Total Number | $\lambda_0 \pm \Delta\lambda$ (nm) | Location[a]/ Type[b] | Rationale |
|---|---|---|---|
| NO / 5 | 230±25 | 0/ L<br>0/ H<br>90/ L<br>90/ H<br>180/ L | Overlaps with Bow 1 and 2, provides full spatial radiance distribution, and accommodates signal levels expected during all parts of the mission. |
| NO (1,0) / 2 | 215±3 | 0/ L<br>0/ H | Used successfully on Bow 1 and 2 to check spectrometer - photometer correlation, and differentiate altitude dependence of NO and OH UV emissions. |
| OH/ 3 | 309±5 | 0/ L<br>0/ H<br>90/ L | Consistent with Bow 1 and 2. |
| Glow features/ 4 | 710.0±2.5<br>540.0±2.5<br>280.0±2.5 | 0/ L<br>0/ L, 90/ L<br>90/ L | Near bands used in Atmospheric Explorer Data experiment; but, avoids atmospheric emission lines. |
| $N_2^+$/ 1<br>CN/ 1 | 391.2±2.5<br>385.0±2.5 | 0/ H<br>0/ H | Seen in ground based measurements - crucial for NASA code validation. |
| O/ 2 | 777.3±2.5 | 0/ L<br>0/ H | Optically thin line for monitoring mechanisms at both high and low altitudes. Provide auxiliary information to 130.4 nm measurements. |
| $NO_2$ / 1 | 620±2.5 | 0/ L | Needed for glow mechanisms, in absence of spectral data. |
| N-I / 1 | 520±2.5 | 0/ L | Horizon/ aspect angle determination and atmospheric emission line. |
| Total 20 | | | |

[a]Location: 0 = on axis, 90 = side-looking, 180 = rear-looking.
[b]Type: L = low signal, minimum $1\times10^{-10}$ W/cm$^2$sr$\mu$m signal
H = high signal, maximum 10 W/cm$^2$sr$\mu$m signal level.

Table 2. Scanning Spectrometer Parameters

| Instrument[a] | Detector | Wavelength Range (nm) | Scan Rates (scan/sec) |
|---|---|---|---|
| VUV | CsI | 115-175 | 0.1/0.53[b] |
| | CsTe | 150-230 | |
| UV | CsTe | 210-330 | 0.1/0.53 |
| | Bialkalai | 270-395 | |
| | Bialkalai | 300-420 | |

[a]Nominal spectral resolution = 1 nm.
[b]Scan rate for the elliptical/ reentry portions of the mission.

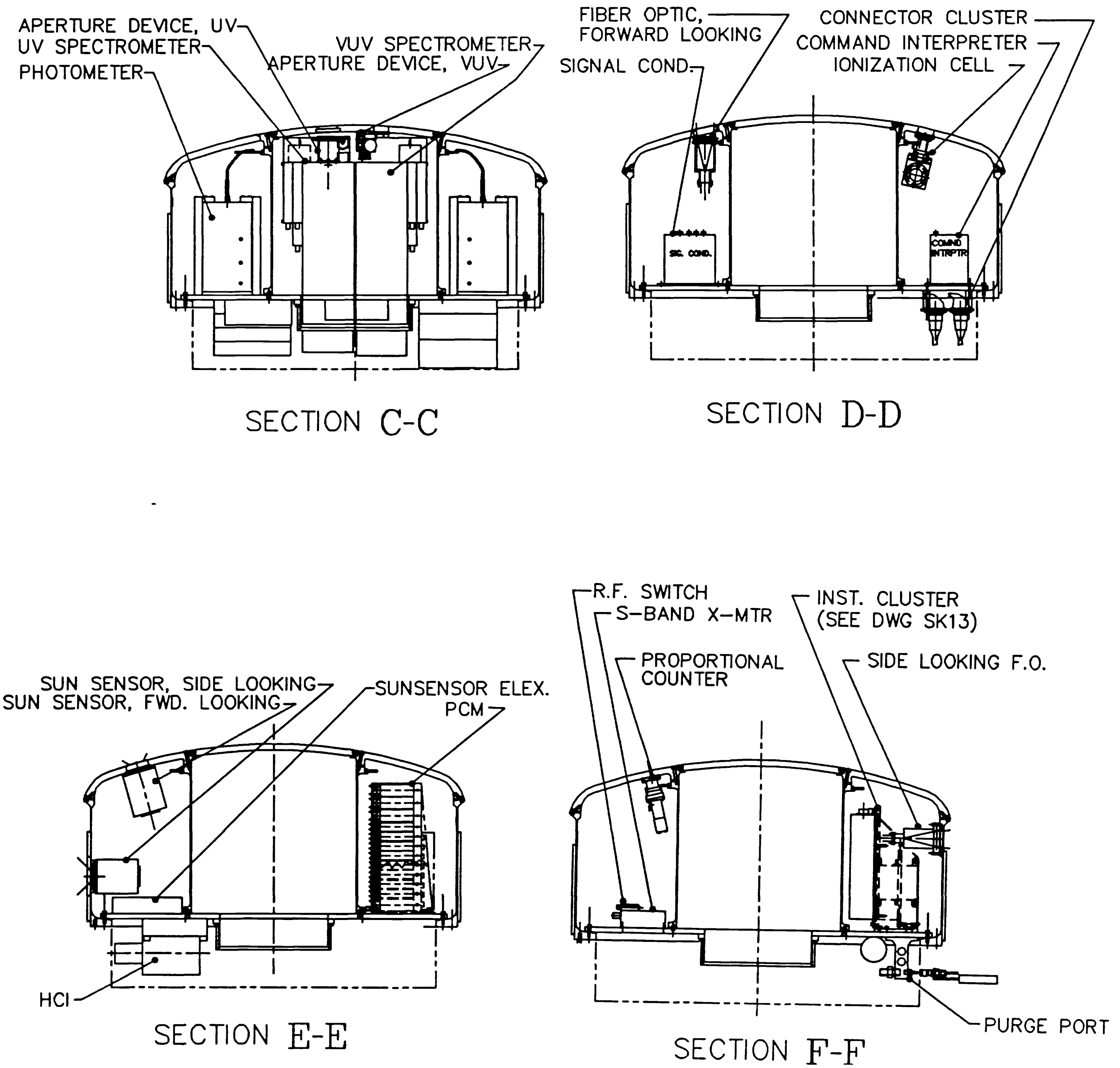


Fig. 11 Plan of the instrument locations, windows, and viewing geometries.

7. Yee, J. H., and Abreu, V. J., "Visible Glow Induced By spacecraft-Environment Interaction," *Geophysical Research Letters*, Vol. 10., No. 2, pp. 126-129, February 1983.
8. G. Caledonia, et al "Mechanistic Investigations of Shuttle Glow", *J. Geoph. Res.,* Vol. 98, No. A3, 3725-3730, Mar. 1 ,1993. and other references therein.
9. G. A Popov and U. Plastinin, "Russian Scientific Radiance Calculations of the Bow Shock III Program", Technical Description of Spacecraft Modifications for the "Bow Shock III" Experiment, Appendix 1, March 1993.
10. G. Candler and R. MacCormack, "The Computation of Hypersonic Ionized Flows in Chemical and Thermal Nonequilibrium," *J. Thermophysics and Heat Transfer*, Vol. 5, No. 3, pp. 266-273, July 1991.
11. I. Boyd and T. Gokcen, "Computation of Axisymmetric and Ionized Flows Using Particle and Continuum Methods", *AIAA Paper No. 93-0729*, Jan. 1993.
12. D. Levin, G. Candler, R. Collins, C. Howlett, P. Espy, E. Whiting, and C. Park, "Comparison of Theory with Atomic Oxygen 130.4 nm Radiation Data from the Bow Shock Ultraviolet 2 Rocket Flight," *AIAA Paper No. 93-2811,* Orlando, Florida, 1993.
13. C. Park "Calculation of Nonequilibrium Radiation in the Flight Regimes of Aero-Assisted Orbital Transfer Vehicles," *Thermal Design of Aero-Assisted Orbital Transfer Vehicles,* ed. H. F. Nelson, Progress in Astronautics and Aeronautics, Vol. 96, 1985.
14. G. F. Karabadzhak, V. D. Peskov, and E. R. Podolyak, "Coordinate Gas Counters with Superhigh Energy Resolution for Plasma Diagnostics," *Nuclear Instruments and Methods,* Vol. .217, pp. 56-64, 1983.